Genetic Deletion of Murine SPRY Domain-Containing SOCS Box Protein 2 (SSB-2) Results in Very Mild Thrombocytopenia

S. L. Masters, K. R. Palmer, W. S. Stevenson, et al. 2005. Genetic Deletion of Murine SPRY Domain-Containing SOCS Box Protein 2 (SSB-2) Results in Very Mild Thrombocytopenia. Mol. Cell. Biol. 25(13):5639-5647. doi:10.1128/MCB.25.13.5639-5647.2005.

MOLECULAR AND CELLULAR BIOLOGY, July 2005, p. 5639–5647 Vol. 25, No. 13
0270-7306/05/$08.00+0 doi:10.1128/MCB.25.13.5639–5647.2005

Genetic Deletion of Murine SPRY Domain-Containing SOCS Box Protein 2 (SSB-2) Results in Very Mild Thrombocytopenia†

S. L. Masters, K. R. Palmer, W. S. Stevenson, D. Metcalf, E. M. Viney, N. S. Sprigg, W. S. Alexander, N. A. Nicola, and S. E. Nicholson*

The Walter and Eliza Hall Institute of Medical Research, 1G Royal Parade, Parkville, 3050 Victoria, Australia

Received 17 January 2005/Returned for modification 12 March 2005/Accepted 5 April 2005

The SSB family is comprised of four highly homologous proteins containing a C-terminal SOCS box motif and a central SPRY domain. No function has yet been ascribed to any member of this family in mammalian species despite a clear role for other SOCS proteins in negative regulation of cytokine signaling. To investigate its physiological role, the murine *Ssb-2* gene was deleted by homologous recombination. SSB-2-deficient mice were shown to have a reduced rate of platelet production, resulting in very mild thrombocytopenia (25% decrease in circulating platelets). Tissue histology and other hematological parameters were normal, as was the majority of serum biochemistry, with the exception that blood urea nitrogen (BUN) levels were decreased in mice lacking SSB-2. Quantitative analysis of SSB mRNA levels indicated that SSB-1, -2, and -3 were ubiquitously expressed; however, SSB-4 was only expressed at very low levels. SSB-2 expression was observed in the kidney and in megakaryocytes, a finding consistent with the phenotype of mice lacking this gene. Deletion of SSB-2 thus perturbs the steady-state level of two tightly controlled homeostatic parameters and identifies a critical role for SSB-2 in regulating platelet production and BUN levels.

The suppressor of cytokine signaling (SOCS) family of proteins contain a central SH2 domain and a homologous 40-amino-acid motif at the C terminus termed the SOCS box (10). CIS was the first SOCS protein identified and was shown to act as a negative regulator of cytokine signaling (33). Studies investigating the genetic deletion of other SOCS proteins in mice highlighted a profound effect on mouse physiology due to their role in suppression of cytokine signaling. For *Socs1*, genetic deletion results in excessive gamma interferon (IFN-γ) signaling, resulting in neonatal death (27). For *Socs3*, complete deletion of the gene is embryonic lethal (25), whereas conditional deletion in adult mice highlights a critical role in interleukin-6 and granulocyte colony-stimulating factor signaling (6, 7). It has previously been determined that the SOCS box interacts with elongins B and C, which can assemble an E3 ubiquitin ligase complex involved in the pathway of proteasomal degradation (34). This mechanism of ubiquitination utilizes a protein complex containing E1, E2, and E3 subunits that, respectively, activate, transport, and ligate ubiquitin. Although the C-terminal SOCS box recruits E3 protein members, the N-terminal domains may interact with the protein targets that are to be degraded (21).

In addition to the family of SOCS proteins that contain an SH2 domain, several other families of SOCS box proteins have now been identified that contain ankyrin, WD40, or other domains (10). The SSB family of proteins contain a SPRY domain N-terminal to a SOCS box. The SPRY domain was originally discovered as a conserved sequence in SPla and RYanodine receptors (23); however, no function has been assigned to the domain in these proteins. The SPRY domain is prevalent in many genomes, with more than 130 proteins known to contain this domain in humans and at least five in yeast (26). The SPRY domain is thought to function as a protein interaction domain. One instance of this is the SPRY domain of RanBPM which specifically binds regions of the androgen receptor (31). More recently the *Drosophila melanogaster* homologue of SSB-1/-4 (Gus) has been shown to interact with the protein Vas, the homologue to the mammalian protein Vasa (29). Vasa has a highly conserved role in the germ cell lineage (24), and male mice lacking the gene for Vasa are sterile (30). In contrast, for *Drosophila*, deletion of Vas leads to female sterility. This is also the case when the gene encoding Gus is mutated and unable to bind Vas (29), and therefore it is possible that mammalian SSB-1/-4 may have a role in the germ cell lineage and in reproduction.

We present here an expression analysis for all four murine SSBs and the phenotypic characterization of mice in which *Ssb-2* has been deleted. SSB-2 is widely expressed including in the kidney, hematopoietic progenitor cells, and megakaryocytes. This is consistent with the phenotype of SSB-$2^{-/-}$ mice, which have a lowered blood urea nitrogen (BUN) level, and thrombocytopenia that most likely results from a decreased rate of platelet production.

MATERIALS AND METHODS

Generation of targeted ES cells for SSB-2-deficient mice. For homologous recombination across the coding region of *Ssb-2*, regions 3′ and immediately 5′ of this region were PCR amplified. Primers were designed to incorporate XhoI (3′ arm) and NotI (5′ arm) restriction enzyme cleavage sites for ligation into the vector pSP:lacZ(NLS)loxNeo (see Table S2 in the supplemental material). The primer for the 5′ end of the 5′ arm also introduced an AscI digestion site to allow linearization of the final construct. These PCR fragments were then ligated into the vector either side of a cassette encoding the genes for β-galactosidase and neomycin resistance (Fig. 2A). The linearized construct was then introduced into C57BL/6 embryonic stem (ES) cells by electroporation and transfected clones were selected in 175 μg of G418 (Invitrogen, Melbourne, Australia)/ml. ES cell

* Corresponding author. Mailing address: The Walter and Eliza Hall Institute of Medical Research, 1G Royal Parade, Parkville, Victoria 3050, Australia. Phone: 61-3-9345-2555. Fax: 61-3-9347-0852. E-mail: snicholson@wehi.edu.au.

† Supplemental material for this article may be found at http://mcb.asm.org/.

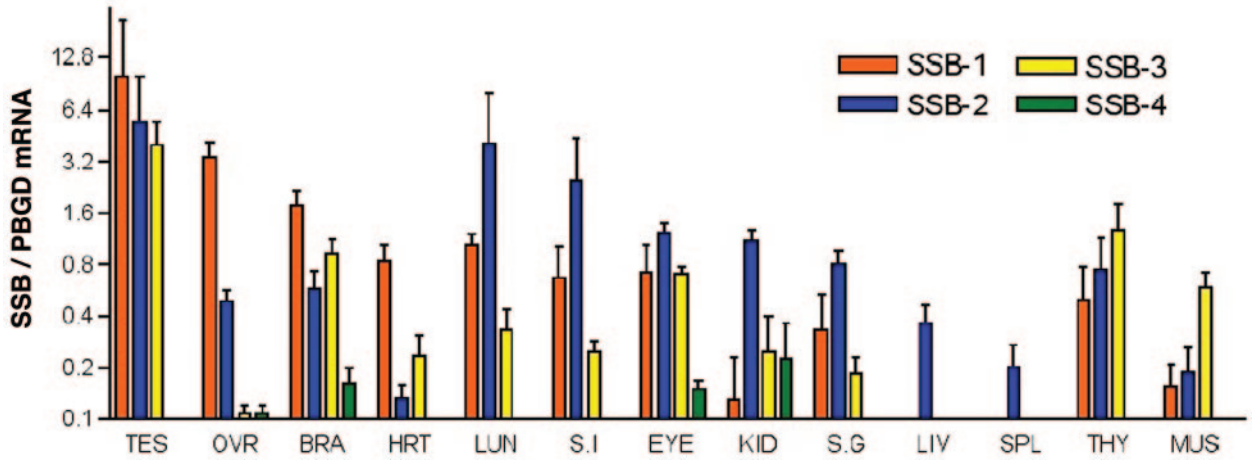

FIG. 1. Expression of SSB mRNA in adult tissues. SSB mRNA levels were quantitated by Q-PCR (normalized against PBGD mRNA levels). All bars represent means and standard deviations for samples derived from three or more individual mice. Abbreviations were used for testes (TES), ovary (OVR), brain (BRA), heart (HRT), lung (LUN), small intestine (S.I), kidney (KID), salivary gland (S.G), liver (LIV), spleen (SPL), thymus (THY), and muscle (MUS).

clones were then screened for homologous recombination of the construct over the targeted region of endogenous *Ssb-2* by Southern analysis of SpeI-digested genomic DNA with a specific PCR fragment of 358 bases directly 3′ of the 3′ arm (Fig. 2B).

Histological analysis and β-galactosidase expression. SSB-2-deficient mice were compared to C57BL/6 wild-type mice matched for age and sex. Peripheral blood was obtained from a minimal (≤200 μl) eye bleed by using a capillary tube and drained into EDTA-coated tubes. Hematological parameters including hematocrit, red and white blood cell counts/volume, and platelet counts/volume were determined by using an ADVIA blood analyzer (ADVIA, Melbourne, Australia). Major organ and tissue weights were recorded before these samples were fixed in 10% buffered formalin and embedded in paraffin. Sections were then stained with hematoxylin and eosin for microscopic analysis. For β-galactosidase histochemistry, tissues were fixed in 4% paraformaldehyde made up in mouse tonicity phosphate-buffered saline (MT-PBS) at 4°C for 1 h. The presence of β-galactosidase was then detected by staining with X-Gal (5-bromo-4-chloro-3-indolyl-β-D-galactopyranoside), which was performed as described previously (12). Tissues were then embedded in paraffin from which sections were prepared, counterstained with nuclear fast red, and examined by light microscopy.

Real-time quantitative PCR (Q-PCR). Total cellular RNA was isolated by using either TRIzol Reagent (Invitrogen) or the RNeasy minikit (Qiagen, Melbourne, Australia) according to the manufacturer's instructions. First-strand cDNA synthesis was performed by using Superscript II RNase H^- reverse transcriptase (Invitrogen). Real-time PCR was performed on an ABI Prism 7900HT sequence detection system (Applied Biosystems, Melbourne, Australia) with forward and reverse primers designed in each instance to cross an intron/exon boundary (see Table S1 in the supplemental material). Cycling conditions were as follows: initial denaturation (95°C for 15 min), followed by 40 cycles of 94°C for 15 s, 50°C (SSB-1 and -4), 60°C (SSB-2, -3, and PBGD), or 49°C (GAPDH) for 30 s and 72°C for 15 s, with a transition rate of 20°C/s and a single fluorescence measurement, a melting curve program (60 to 95°C, with a heating rate of 0.1°C/s and continuous fluorescence measurement), and a final cooling step to 40°C. All PCRs were performed by using the QuantiTect SYBR Green PCR Kit (Qiagen). The specificity of the SYBR green reaction was assessed by melting point analysis and gel electrophoresis. SSB mRNA levels were quantified from standard curves by using SDS 2.2 software (Applied Biosytems) and are presented as arbitrary units standardized against either porphobilinogen deaminase (PBGD) or glyceraldehyde-3-phosphate dehydrogenase (GAPDH) mRNA. GAPDH was used for analysis of hematopoietic samples for which PBGD levels were low relative to the gene of interest. Standard curves were generated by using dilutions of an oligonucleotide corresponding to the amplified fragment.

Immunoprecipitation and Western blotting. Rabbit polyclonal antibodies recognizing murine SSB-2 were generated by immunizing a rabbit with purified recombinant SSB-2 protein (32). The same protein was also coupled to NHS (*N*-hydroxysuccinimide)-activated Sepharose (Amersham Biosciences, Sydney, Australia) according to the manufacturer's instructions and used to purify antibodies from immune serum. Affinity-purified anti-SSB2 antibodies were either conjugated to NHS-Sepharose at 1.5 mg/ml or biotinylated by using sulfo-NHS-Biotin (Pierce, Rockford, IL) according to the manufacturer's instructions. Protein lysates were generated from tissues as described previously (14) and precleared with ethanolamine-blocked NHS-activated Sepharose (100 μl). Proteins were then immunoprecipitated from tissue lysates by using anti-SSB-2 antibodies coupled to Sepharose (30 μl) and separated by sodium dodecyl sulfate-polyacrylamide gel electrophoresis under reducing conditions. Proteins were then electrophoretically transferred to polyvinylidene difluoride membranes (Hybond-P; Amersham Biosciences) and blocked overnight in 10% (wt/vol) skim milk prior to incubation with 0.15 μg of biotinylated anti-SSB-2 antibodies/ml. Antibody binding was visualized with horseradish peroxidase-conjugated streptavidin (Chemicon, Melbourne, Australia) and the enhanced chemiluminescence system (Amersham Biosciences).

FACS. Single-cell suspensions were made by passing spleen, lymph node, or thymus tissues through a fine sieve. Where necessary, red blood cells were lysed (9) prior to incubation of the suspension with primary antibodies as described previously (28). All fluorescence-activated cell sorting (FACS) antibodies were obtained from Pharmingen (San Diego, CA). For analysis of peripheral hematopoietic subsets, the primary antibodies used were rat antibodies that were directly conjugated to fluorochromes (fluorescein isothiocyanate [FITC]-CD4, FITC-Thy1, phycoerythrin [PE]-CD8, PE-B220, and PE-Mac1). To examine bone marrow hematopoietic progenitor cells, a cocktail of FITC-conjugated lineage markers (B220, CD3, CD4, CD5, CD8, DX5, Gr-1, Mac1, NK1.1, and Thy1) was used to distinguish non-lineage-committed cells (Lin^{-ve}), and then a population enriched for hematopoietic progenitor cells was detected by using a biotinylated c-Kit antibody detected with APC-streptavidin. For visualization of β-galactosidase expression, the fluorogenic substrate fluorescein di-β-D-galactopyranoside (FDG) was used. A 20-μl aliquot of antibody-stained cells was hypertonically labeled with FDG at 37°C for 120 s, and the reaction was stopped by the addition of 400 μl of cold buffered saline solution (BSS) plus 10% fetal calf serum (Sigma). Before flow cytometric analysis, 1 μg of propidium iodide (PI)/ml was added to enable dead cell detection and exclusion. Cells were finally analyzed by using a fluorescence-activated cell scanner (LSR; BD Biosciences, Sydney, Australia).

Purification of peripheral hematopoietic populations. Peripheral hematopoietic populations were purified for analysis by Q-PCR. T cells were purified from lymph nodes by using a T-cell enrichment column according to manufacturer's instructions (R&D Systems, Minneapolis, MN). Splenic cell suspensions were prepared as for flow cytometry. Purification of B cells from these suspensions was performed with biotinylated B220 antibody (Pharmingen) and streptavidin-coated beads (Dynal, Oslo, Norway). After red blood cell lysis, peripheral blood monocytes were purified from whole blood by FACS sorting $Gr\text{-}1^{+ve}$ $Mac1^{+ve}$ cells. Bone marrow macrophages were obtained by culture of whole bone marrow in the presence of M-CSF as described previously (6).

Agar cultures. Formation of colonies from SSB-2 deficient and wild-type bone marrow was determined by culture in semisolid agar. Colony type and number in response to cytokine stimulation was analyzed as described previously (12). To

determine whether cells giving rise to colonies in response to the cytokine normally expressed SSB-2, the bone marrow was first fractionated according to high, medium, and low β-galactosidase expression by using flow cytometry as described above.

Serum analysis. Peripheral blood was obtained from a minimal (≤200 μl) eye bleed by using a capillary tube. The blood was then allowed to clot at room temperature for 2 h before being clarified by centrifugation at 3,000 rpm. Serum biochemical analyses were performed by the IDEXX Central Veterinary Diagnostic Laboratories (Melbourne, Australia). Serum TPO levels were determined by enzyme-linked immunosorbent assay according to the manufacturer's instructions (R&D Systems).

CFU-spleen (CFU-S) analysis. SSB-2-deficient and wild-type bone marrow was injected via the tail vein of irradiated C57BL/6 mice according to established protocols (13). At day 12 the spleens were placed in Carnoy's solution (60% [vol/vol] ethanol, 30% [vol/vol] chloroform, 10% [vol/vol] acetic acid), and visible colonies were counted.

Platelet half-life. Biotinylation of platelets was performed as described previously (3). Briefly, sulfo-NHS-biotin (30 mg/kg in 200 μl of MT-PBS) was injected via the tail vein. Platelets were obtained for analysis at various time points from a small (~2-μl) aliquot of blood taken from the tail vein into buffered saline citrate glucose solution (BSCG; 1.6 mM KH_2PO_4, 8.6 mM NaH_2PO_4 [pH 6.5], 129 mM NaCl, 13.6 mM sodium citrate, 11.1 mM glucose). Platelets were then washed in BSS containing 2% FCS and centrifuged at 1,300 × *g* for 10 min at room temperature before being resuspended in the same medium. Platelets were then stained with FITC-CD41 antibody and PE-streptavidin (Pharmingen) by incubation for 30 min on ice. The platelets were then washed before being resuspended in BSCG with 1 μl of PI/ml to identify dead cells. Samples were analyzed by flow cytometry, where platelets were identified as FITC positive and by their size, and then the percentage of these that were biotinylated (PE^{+ve}) was assessed.

Analysis of megakaryocyte ploidy. Megakaryocyte ploidy was determined as described previously (11). Essentially, bone marrow was harvested from femurs and tibias into 1 ml of ice-cold CATCH (calcium-free, magnesium-free Hanks balanced salt solution with 1 mM adenosine; 2 mM theophylline; 0.38% [wt/vol] sodium citrate; 2% [wt/vol] bovine serum albumin) and filtered through a 100-μm-pore-size filter. Then, 2 μl of FITC-CD41 antibody was added for 30 min prior to hypertonic loading with 3 ml of PI (0.05 mg/ml in 0.1% sodium citrate) for 1 h. Cells were then washed twice with 20 ml of CATCH by centrifugation at 400 × *g* for 5 min, and RNase was added to a concentration of 50 μg/ml for 30 min at room temperature. Flow cytometry was then performed as described previously (11). Megakaryocytes were identified as $FITC^{+ve}$, and ploidy was determined on the basis of PI staining.

RESULTS

Quantitative expression of SPRY domain-containing SOCS box (SSB) mRNA. There are four murine SSB proteins, and these are highly conserved. Sequence alignment (2) showed that SSB-1 and -4 are the most homologous (84% similar) and that SSB-2 and -3 share the least homology (42% similar). Given the close amino acid homology of SSB proteins, we were interested in determining their pattern of expression. An overlapping expression pattern may indicate functional redundancy, whereas expression of a singular SSB may highlight a unique functional role. We therefore examined SSB mRNA levels in a variety of adult tissues by Q-PCR. SSB-1, -2, and -3 were ubiquitously expressed across a panel of 14 tissues; however, SSB-4 was only ever present at a relatively low level (Fig. 1) and was not detectable by Northern analysis (data not shown). SSB-1, -2, and -3 were all most highly expressed in the testes at relatively similar levels. Comparable expression of these SSBs was also observed in the eye and thymus. In contrast, expression of SSB-1 was predominant in the ovary and heart, SSB-2 was predominant in the lung, kidney, liver, and spleen, and SSB-3 was predominant in muscle (Fig. 1).

Generation of SSB-2-deficient mice. To elucidate a physiological role for SSB-2, the gene coding for this protein was

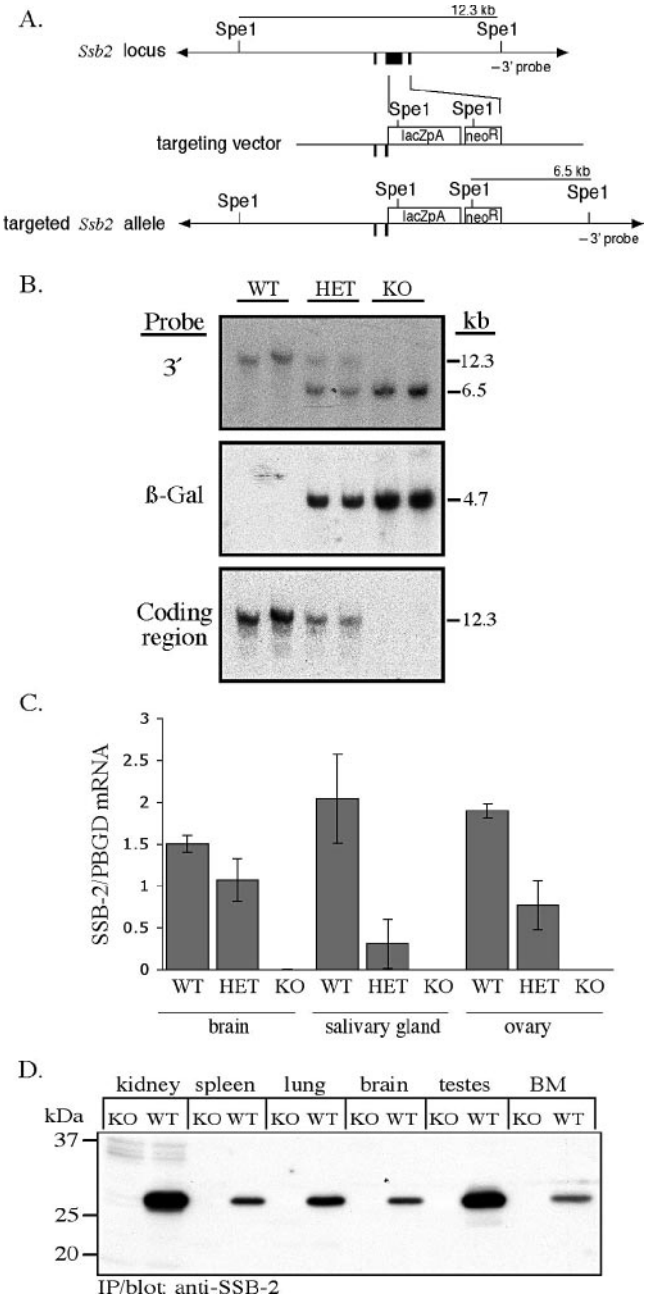

FIG. 2. Disruption of *Ssb-2* by homologous recombination. (A) The exons for *Ssb-2* are shown in black (top). The targeting vector (middle) replaces the entire coding region with the β-galactosidase PGKneo cassette (bottom). (B) Southern blot analysis of SpeI-digested genomic DNA from the tails of mice derived from a cross between $SSB\text{-}2^{+/-}$ mice. The blot was hybridized with the 3′ *Ssb-2* genomic probe, which distinguishes between endogenous (12.3-kb) and targeted (6.5-kb) alleles (top panel). The blot was then hybridized with a 266-bp probe corresponding to the coding region for β-galactosidase (center panel) and an 833-bp probe corresponding to the coding region for SSB-2 (bottom panel). (C) Expression of SSB-2 mRNA as measured by Q-PCR in tissues of wild-type (WT), $SSB\text{-}2^{+/-}$ (HET), and $SSB\text{-}2^{-/-}$(KO) mice. SSB2 mRNA levels were normalized against PBGD mRNA levels. All bars represent averages and standard deviations for samples derived from three mice. (D) Lysates (1 mg of protein, except for bone marrow [BM; 0.36 mg]) from a variety of wild-type and $SSB\text{-}2^{-/-}$ tissues were analyzed by immunoprecipitation (IP) with anti-SSB-2 antibodies and Western blotting with biotinylated SSB-2 antibodies.

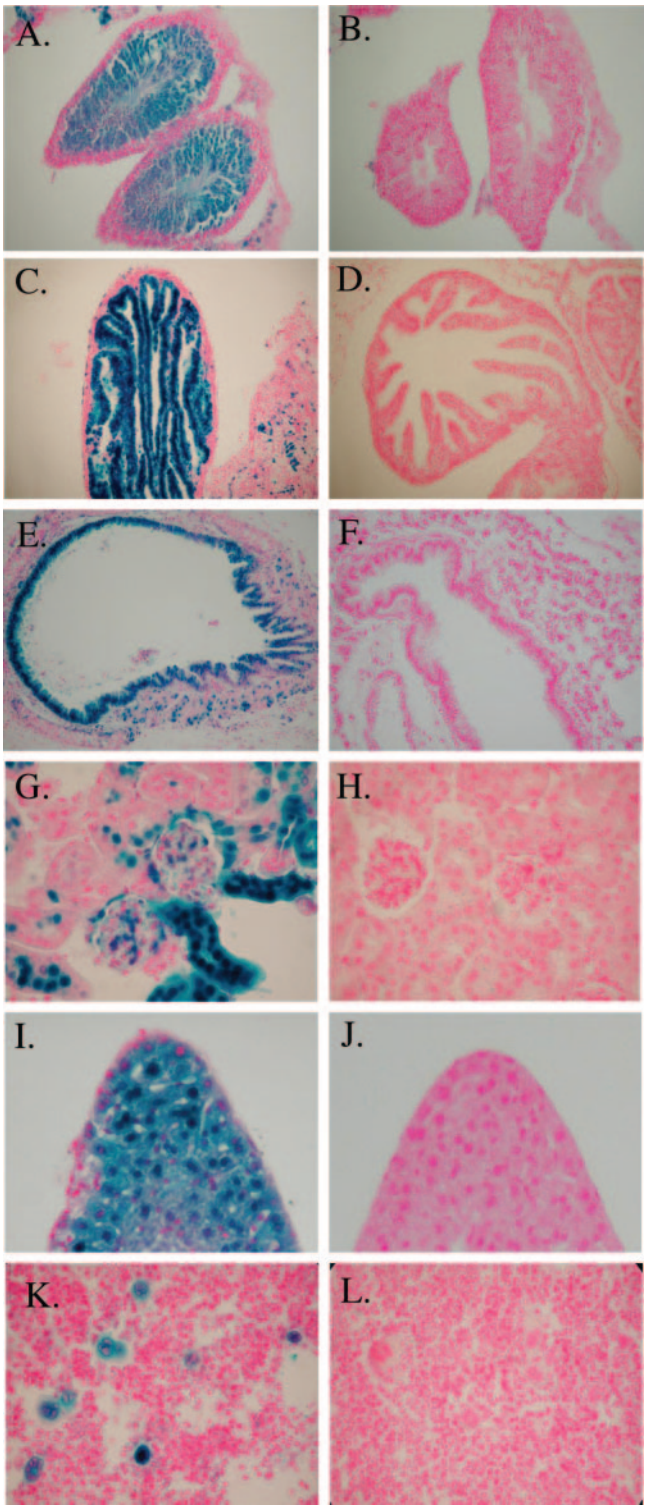

FIG. 3. β-Galactosidase histochemistry of SSB-2-deficient mice. β-Galactosidase staining (blue) in tissues from SSB-$2^{-/-}$ mice (left) can be compared to that in wild-type littermates (right). Sections were counterstained in nuclear fast red and photographed at ×20 magnification, except for kidney, liver, and bone marrow. which were photographed at a ×60 magnification. (A and B) Testes; (C and D) fallopian tube; (E and F) lung; (G and H) kidney; (I and J) liver; (K and L) bone marrow.

TABLE 1. Parameters for blood serum and whole blood from wild-type and SSB-$2^{-/-}$ mice[a]

Parameter	Value for mice (mean ± SD)	
	WT	KO
Whole blood		
WBC (10^3 cells/μl)	7.9 ± 2.3	7.0 ± 2.3
RBC (10^6 cells/μl)	11.0 ± 0.5	11.0 ± 0.3
Hb (g/dl)	16.9 ± 0.5	16.5 ± 0.5
PLT* (10^9 cells/liter)	1338 ± 78	966 ± 130
MPV (fl)	6.8 ± 0.9	6.9 ± 1.3
PDW (%)	49.0 ± 5.2	51.6 ± 9.4
Blood serum		
Sodium (mmol/liter)	77.7 ± 1.7	81 ± 1.7
Potassium (mmol/liter)	3.2 ± 0.1	2.8 ± 0.2
Chloride (mmol/liter)	59 ± 1	61 ± 1.7
Urea** (mmol/liter)	9.4 ± 1.5	7.2 ± 1.0
Creatinine	0.04 ± 0.01	0.04 ± 0.01
Albumin (g/liter)	41.7 ± 2.1	41 ± 3.0
Total bilirubin (μmol/liter)	2.3 ± 0.6	2.7 ± 2.1
ALP (IU/liter)	182 ± 24	207 ± 95
AST (IU/liter)	79 ± 14	117 ± 18
CK (IU/liter)	277 ± 180	247 ± 33

[a] White cell count (WBC), red blood cell count (RBC), hemoglobin (Hb), platelet count (PLT), mean platelet volume (MPV), platelet distribution width (PDW), alkaline phosphatase (ALP), aspartate aminotransferase (AST), and creatine kinase (CK) values were determined. Values are for at least four mice except for ALP, AST, and CK, which are for two or more mice. *, $P \leq 0.0001$; **, $P \leq 0.0003$. WT, wild type; KO, knockout.

deleted by homologous recombination. A construct was designed to delete the entire region coding for SSB-2 and also place expression of the β-*galactosidase* gene under control of the endogenous *Ssb-2* promoter (Fig. 2A). Transfection of the construct into C57BL/6 ES cells was found to result in successful recombination by Southern blot of total ES cell genomic DNA in 11 of 225 clones (data not shown). Targeted ES cells were then injected into blastocysts to generate chimeric mice and hence F_1 mice heterozygous for the *Ssb-2* deletion. Germ line transmission was confirmed for two independent clones. Homologous recombination of the construct across the targeted region of *Ssb-2* to delete the *Ssb-2* coding region was confirmed by Southern blot of genomic DNA (Fig. 2B). To confirm deletion of *Ssb-2*, mRNA and protein levels were examined in SSB-$2^{-/-}$ mice. As determined by Q-PCR, no transcript was detected in SSB-$2^{-/-}$ tissues, and approximately half the amount of transcript was observed in tissues from SSB-$2^{+/-}$ mice (Fig. 2C). Furthermore, the absence of SSB-2 protein from adult mouse tissues was confirmed by immunoprecipitation and Western blotting, where a band of 28 kDa corresponding to SSB-2 was observed in wild-type but not SSB-$2^{-/-}$ tissues (Fig. 2D). Matings of SSB-2 heterozygous male and female mice revealed that all three resulting genotypes were born at the expected Mendelian frequency (data not shown). Both male and female mice homozygous for the deletion of SSB-2 were fertile.

Histology and β-galactosidase expression in SSB2$^{-/-}$ mice. SSB-2 expression as determined by Q-PCR was relatively ubiquitous (Fig. 1). We therefore took advantage of the β-galactosidase expression cassette that had been inserted under the control of the *Ssb-2* promoter as a surrogate marker for expression. This has the added advantage of revealing the prob-

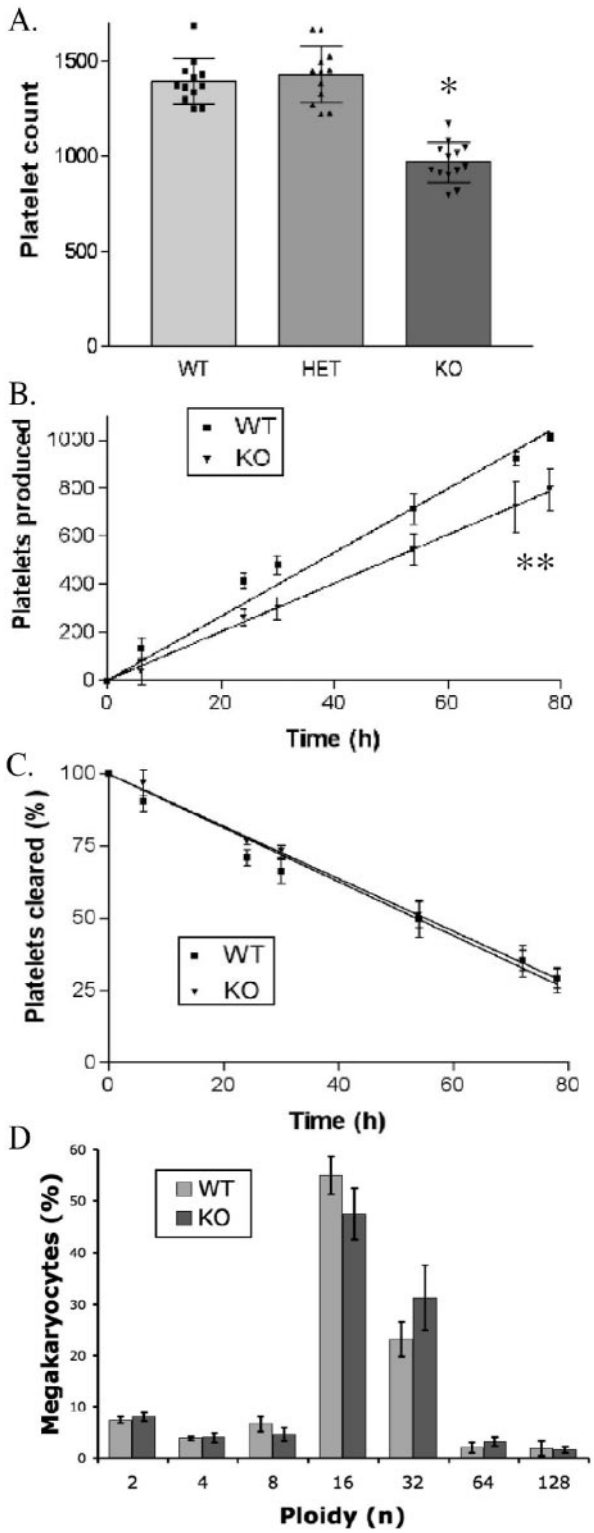

FIG. 4. Analysis of SSB-$2^{-/-}$ platelets and megakaryocytes. (A) Blood platelet counts (10^9 cells/liter) for 12 or more mice (mean ± the standard deviation) of each genotype: SSB-$2^{+/+}$ (WT), SSB-$2^{+/-}$ (HET), and SSB-$2^{-/-}$ (KO) mice. ✻, $P \leq 0.0001$. (B) Platelet production as determined by in vivo biotinylation. Platelets were analyzed by flow cytometry with PE-streptavidin and FITC-CD41 antibody to determine the absolute number of unlabeled platelets ($PE^{-ve}/FITC^{+ve}$) produced over time. The number of platelets at each time point is the mean ± the standard deviation for three mice. ✻✻, $P \leq 0.001$. (C) The percentage of labeled platelets cleared over time as determined by flow cytometry ($PE^{+ve}/FITC^{-ve}$) after in vivo biotinylation. (D) Analysis of megakaryocyte ploidy in SSB-$2^{-/-}$ mice. Megakaryocytes were identified as FITC-CD41 positive, and their DNA was quantitated by hypertonic labeling with PI. The average percentage of each ploidy peak (as measured by PI labeling) is shown for four mice of each genotype. n, number of sets of chromosomes.

able cellular distribution of SSB-2. Histological examination of SSB-$2^{-/-}$ mice tissues revealed no overt differences compared to wild-type littermates. Almost all SSB-$2^{-/-}$ organs and tissue types showed evidence of β-galactosidase expression, and this correlated with expression as determined by Q-PCR. In the reproductive organs, β-galactosidase expression was seen in both mature and immature sperm within the testes (Fig. 3A) and in the epithelial lining of the fallopian tubes (Fig. 3C). In other organs, subsets of cells expressed β-galactosidase, especially within the pancreas and salivary glands and less so within the cerebellum and muscle (data not shown). Staining was also intense in several cell types with high turnover rates, e.g., vascular endothelial cells, skin keratinocytes, and villi in the small intestine (data not shown). Other villi and microvilli expressed β-galactosidase, including those of the bronchioles in the lung (Fig. 3E) and those in the proximal and distal convoluted tubules of the kidney (Fig. 3G). Expression of β-galactosidase within the liver was relatively ubiquitous (Fig. 3I). Within hematopoietic tissues, lymphocytes did not appear to express β-galactosidase; however, it is thought that sporadic silencing of this gene can occur in these populations (22). In contrast, megakaryocytes in the bone marrow and spleen were strikingly positive for β-galactosidase expression (Fig. 3K). Staining was not observed in wild-type tissues that had been processed in parallel (Fig. 3B, D, F, H, J, and L).

Decreased platelet formation in SSB-2-deficient mice. Because of the marked expression of SSB-2 in megakaryocytes (Fig. 3K), analysis of platelets and megakaryocytes in SSB-2-deficient mice was performed. Most peripheral blood parameters including red and white blood cell counts, volumes, and hematocrit were unaltered (Table 1). However, SSB-2-deficient mice displayed a consistent 25% decrease in platelet count compared to both wild-type mice and mice heterozygous for the deletion of SSB-2 (Fig. 4A). Thrombocytopenia of similar severity was also observed in SSB-$2^{-/-}$ mice generated from an independently targeted ES cell clone [SSB-$2^{-/-\ (421)}$ platelet count of (1,088 ± 221) × 10^9 cells/liter compared to wild-type platelets at (1,314 ± 202) × 10^9 cells/liter; $n = 11$, $P = 0.01$]. The average platelet volume was not increased (Table 1), and SSB-$2^{-/-}$ platelets appeared normal by electron microscopy (data not shown). Possible explanations for a decreased platelet count include (i) a decrease in megakaryocyte numbers, (ii) lowered production rate of platelets from the same number of megakaryocytes, or (iii) increased clearance of platelets. To address these issues, several experiments were performed. As determined by light microscopy (megakaryocytes per 10 high-powered fields), the appearance, location, and number of megakaryocytes in bone marrow from the femur and sternum appeared to be normal: 64.8 ± 11.0 for wild-type mice compared to 62.8 ± 7.1 for SSB-$2^{-/-}$ mice. To assess whether the decrease in circulating platelets was due to alterations in

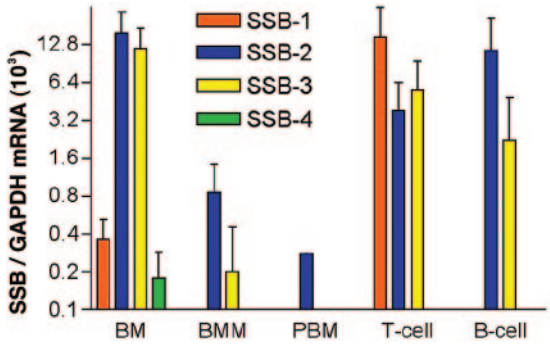

FIG. 5. Expression of SSB family members in hematopoietic cell lineages. (A) SSB mRNA levels have been normalized against GAPDH mRNA. Bars represent means ± the standard deviations. The results for whole bone marrow (BM; $n = 4$), bone marrow-derived macrophages (BMM; $n = 3$), peripheral blood macrophages (PBM; $n = 1$), peripheral lymph node T cells ($CD3^{+ve}$) ($n = 3$), and splenic B cells ($B220^{+ve}$) ($n = 3$) are shown.

production or clearance, platelet half-life was analyzed in vivo. Platelet biotinylation was performed, and the presence of labeled platelets monitored by flow cytometry. No obvious difference in the clearance rate of platelets was observed (Fig. 4C). By plotting the number of unlabeled platelets produced against time (Fig. 4B), it was found that the SSB-$2^{-/-}$ mice produced fewer platelets per hour ([13.2 ± 0.3 platelets/h] × 10^9 cells/liter for wild-type mice compared to [10.1 ± 0.3 platelets/h] × 10^9 cells/liter for SSB-$2^{-/-}$ mice; $P \leq 0.001$).

To complement this finding, analysis of megakaryocyte ploidy was also performed, and although a moderate increase in ploidy was observed this was not statistically significant (Fig. 4D). Thrombopoietin (TPO) is a key regulator of megakaryocyte and platelet formation (1); however, the level of TPO in serum was not significantly different between wild-type (4,157 ± 682 pg/ml) and SSB-$2^{-/-\ (421)}$ (3,608 ± 814 pg/ml) mice ($n = 11$, $P = 0.14$). Therefore, the 25% platelet decrease in SSB-$2^{-/-}$ mice appears to be due to the production of fewer platelets per megakaryocyte.

Normal hematopoiesis in SSB-2-deficient mice. To further explore the expression of SSBs in hematopoietic lineages, various populations were examined by Q-PCR. Expression of SSB-2 and SSB-3 mRNA was found to be predominant in total bone marrow and T and B cells (Fig. 5). SSB-1 mRNA was most highly expressed in T cells, whereas SSB-4 expression was almost undetectable. For SSB-$2^{-/-}$ mice the distribution of hematopoietic lineages in peripheral organs was determined by differential counting (bone marrow) or by flow cytometric analysis with specific antibodies (spleen, thymus, lymph nodes, and peritoneal cavity) (Table 2). No differences were observed between SSB$2^{-/-}$ mice and wild-type littermates.

To examine expression of SSB-2 in hematopoietic progenitor cells, bone marrow was fractionated by FACS sorting according to the level of β-galactosidase expression (low, 73% of bone marrow; medium, 21% of bone marrow; and high, 6% of bone marrow from SSB-$2^{-/-}$ mice). These fractions were then tested in vitro for their capacity to produce colonies in response to specific cytokines. Colony-forming cells were enriched in the fraction of bone marrow cells expressing high β-galactosidase levels (Table 3), suggesting that the SSB-2 promoter is active in the hemopoietic progenitor compartment. Furthermore, bone marrow that had been enriched for progenitor cells with specific antibodies (Lin^{-ve}/$ckit^{+ve}$) (Fig. 6A) showed that, excluding megakaryocytes, hemopoietic progenitors had the highest level of expression of SSB-2 in the bone marrow, as assessed by both β-galactosidase and Q-PCR (Fig. 6B). Stimulation of SSB-$2^{-/-}$ bone marrow cells by a range of cytokines revealed no difference in colony formation compared to wild-type mice with respect to the number, composition, or lineage of colonies (Table 4). Similarly, no difference was seen between wild-type and SSB-$2^{-/-}$ bone marrow with respect to CFU-S numbers (19 ± 6.2 colonies per spleen compared to 18.7 ± 2.1 colonies per spleen, respectively [$n = 3$]).

Increased clearance of BUN from SSB-$2^{-/-}$ serum. From a spectrum of blood metabolic parameters reflecting kidney and liver function (Table 1), only the BUN level was significantly different between wild-type and SSB-2-deficient mice. The BUN level was decreased by 23% in SSB-$2^{-/-}$ mice ($P \leq 0.0003$), whereas mice heterozygous for the deletion of SSB-2 had an intermediate phenotype (14% lower) (Fig. 7). Urine from SSB-$2^{-/-}$ mice was analyzed by SDS-PAGE with Coomassie blue staining, but no difference was observed with regard to protein composition (data not shown).

TABLE 2. Distribution of hematopoietic lineages in SSB-$2^{-/-}$ and wild-type mice as determined by differential counting and FACS analysis[a]

Evaluation and cell type	% Value for mice ± SD	
	WT	KO
Bone marrow differential		
Blasts	2.3 ± 0.6	5.3 ± 2.5
Promyelocytes/myelocytes	8.3 ± 2.3	3.7 ± 2.3
Metamyelocytes/neutrophils	35.3 ± 3.1	35.3 ± 6.4
Lymphocytes	22.7 ± 3.1	22.5 ± 4.5
Monocytes	6.7 ± 3.5	6.3 ± 2.1
Eosinophils	2.3 ± 1.2	3.3 ± 1.6
Nucleated erythroid cells	22.3 ± 8.1	23.3 ± 4.0
FACS analysis		
Spleen		
CD4	10.4 ± 2.5	9.2 ± 1.7
CD8	18 ± 2.3	18.6 ± 1.6
Mac1	3.2 ± 1.2	3 ± 0.6
Thymus		
CD4	87.3 ± 1.1	85.8 ± 4
CD8	86.3 ± 5.9	82.7 ± 5.3
CD4/CD8	89.3	90
Lymph node		
CD4	24.3 ± 9.2	24.3 ± 11.8
CD8	15.3 ± 6.2	18.8 ± 9.4
CD4/CD8	0.7 ± 0.4	0.7 ± 0
B220	20 ± 10.9	27.6 ± 13
Thy-1	38.8 ± 24.4	47.2 ± 25.4
Peritoneal cavity		
Mac1	18.15 ± 8.6	16.5 ± 0.1
B220	60.0 ± 1.5	61.0 ± 2.0

[a] Values are for at least three mice, except for thymus CD4/CD8, which is the average for two mice. WT, wild type; KO, knockout.

TABLE 3. Colony formation from SSB-2$^{-/-}$ bone marrow fractions in response to cytokine stimulation[a]

BM fraction	Stimulus[b]	No. of colonies formed					
		B	G	GM	M	Eo	Meg
Low	GM-CSF		0	0	1	0	
	G-CSF		1	0	0		
	IL-3	0	0	0.5	0	0	0
	M-CSF		0	0	1		
	SCF	0	0	0	0		
	SCF + IL-3 + EPO	0	0	1	0	0	0
Medium	GM-CSF		4	1	3.5	0	
	G-CSF		2	0	0		
	IL-3	1.5	2	0.5	6	0	1.5
	M-CSF		0	1	6		
	SCF	1.5	2.5	1	0		
	SCF + IL-3 + EPO	8	6.5	5.5	7	0.5	6
High	GM-CSF		22.5	15	36	1.5	
	G-CSF		13.5	0	2		
	IL-3	9	26	13.5	33.5	1	7.5
	M-CSF		3.5	6.5	66		
	SCF	14.5	35	1.5	2.5		
	SCF + IL-3 + EPO	16	22	26.5	29	0	22

[a] Fractions were determined according to high, medium, or low levels of β-galactosidase expression. A total of 10,000 cells in agar culture were stimulated by the cytokines listed, and colonies were enumerated after 7 days. Colonies were identified as blast (B), granulocyte (G), granulocyte/macrophage (GM), macrophage (M), eosinophil (Eo), or megakaryocyte (Meg). Values are averages from two independent experiments.

[b] GM-CSF, granulocyte-macrophage colony-stimulating factor; G-CSF, granulocyte colony-stimulating factor; IL-3, interleukin-3; SCF, stem cell factor; EPO, erythropoietin.

TABLE 4. Analysis of whole bone marrow from SSB-2$^{-/-}$ and wild-type mice as determined by colony assay formation in response to cytokine stimulation[a]

Mouse type and stimulus[b]	No. of colonies formed					
	B	G	GM	M	Eo	Meg
WT						
GM-CSF		17.5	10	22	1.5	
G-CSF		11	0	0		
M-CSF		3	4.5	58.5		
IL-3	5	15.5	11.5	13	1	7
EPO						8
SCF	3.5	13.5	1	1		0
TPO						2.15
SCF + IL-3 + EPO	5.5	15.5	15	16.5	0.5	25
IL-6		8.5	0.5	1.5		2
KO						
GM-CSF		12.5	3.5	25	1.5	
G-CSF		5.5	0.5	0		
M-CSF		1.5	3	44		
IL-3	3.5	11.5	12	15.5	0.5	6
EPO						4.5
SCF	4	12	0.5	0.5		0
TPO						2
SCF + IL-3 + EPO	7	17.5	9.5	13.5	0.5	18.5
IL-6		7.5	0	0.5		

[a] A total of 25,000 cells in agar culture were stimulated by the cytokines listed, and colonies were enumerated. Colonies were identified as blast (B), granulocyte (G), granulocyte/macrophage (GM), macrophage (M), eosinophil (Eo), or megakaryocyte (Meg). Values are averages from two independent experiments.

[b] See Table 3, footnote *b*. KO, knockout; WT, wild type.

DISCUSSION

The deletion of murine SSB-2 in the present study represents the first physiological analysis of a mammalian SSB. This deletion was observed to perturb at least two biological processes. First, it resulted in thrombocytopenia. Second, it lowered the BUN level in these mice. Although the absolute decrease in platelet count was modest, this is a homeostatic parameter that is tightly regulated (5, 15, 16, 18). Also, some proplatelet cytokines only generate small increases in platelet counts in vivo (19, 20). With these points in mind, a 25% decrease in platelet count can be regarded as physiologically significant. Our findings show that there is a production defect in SSB-2$^{-/-}$ animals whereby the number of platelets derived from the same number of steady-state megakaryocytes is fewer than for wild-type animals. This is consistent with high SSB-2 expression in megakaryocytes, as assessed by determining the β-galactosidase activity under the endogenous *Ssb-2* promoter. If indeed SSB-2 functions as other SOCS box proteins to degrade target proteins, then deletion of SSB-2 may result in the increased activity or abundance of an inhibitor of platelet formation. Despite clear expression of SSB-2 in progenitor cell populations, deletion of SSB-2 did not alter the formation of hematopoietic colonies as studied in vitro or the distribution of any hematopoietic lineages studied. From these experiments, we conclude that thrombocytopenia due to SSB-2 deficiency does not appear to result from defects in megakaryocyte progenitors or the production of megakaryocytes.

BUN levels were decreased by 23% in SSB-2$^{-/-}$ mice and by 14% in SSB-2$^{+/-}$ mice. This indicates that, in contrast to the thrombocytopenia in these animals, the decrease in BUN is

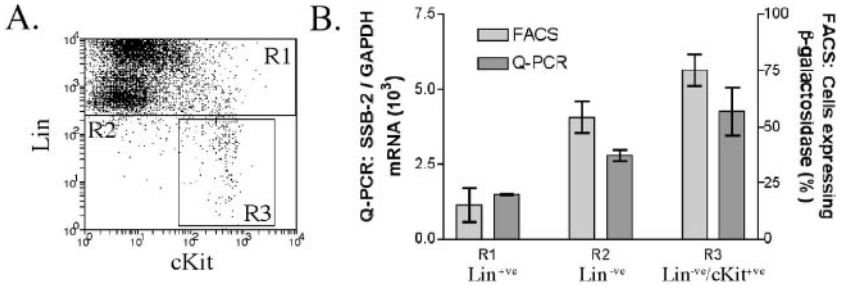

FIG. 6. Expression of SSB-2 in hematopoietic stem cells. (A) SSB-2$^{-/-}$ bone marrow was separated into lineage-committed (Lin^{+ve}; R1), lineage-undefined (Lin^{-ve}; R2), and hematopoietic (Lin^{-ve}/cKit^{+ve}; R3) stem cells by FACS. (B) These fractions were then analyzed by using β-galactosidase as a marker of SSB-2 expression and by Q-PCR detection of SSB-2 mRNA levels normalized against GAPDH. Values are means ± the standard deviations for three mice.

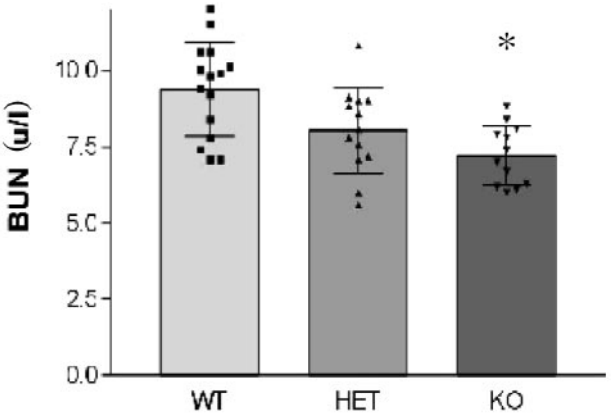

FIG. 7. BUN level in SSB-$2^{-/-}$ mice. BUN levels were measured for wild-type (WT), SSB-$2^{+/-}$ (HET), and SSB-$2^{-/-}$ (KO) mice (n = 11). *, $P \leq 0.0001$.

Ssb-2 gene dosage dependent. This phenotype could be due to perturbations of hydration, liver function, or kidney function (4, 8, 17). Liver function in SSB-$2^{-/-}$ mice did not appear to be compromised because the livers in these mice had normal histology, and metabolic parameters reflecting liver function were unchanged. There was no circumstantial evidence (such as a decrease in other related serum parameters) to suggest that hydration was the cause of this phenotype. A high level of SSB-2 expression was observed in the proximal/distal tubules of the kidney, consistent with SSB-2 action leading to an increased removal of urea at a steady state.

The *Drosophila* homologue of SSB-1/-4 (Gus) (29) has been shown to interact with Vas, a protein that is required for female fertility and has a known role maintaining germ cell morphology (24). Mutation of Gus leads to germ cell malfunction and female sterility in *Drosophila* (29). The possibility that mammalian SSB-1 or -4 interact with the mammalian Vasa homologue (MVH) remains to be tested. Interestingly, expression analysis showed that SSB-4 was not expressed at a significant level in adult tissues. Furthermore, SSB-1 was expressed very highly in the testes and almost eight times more highly than any other SSB in the ovary. This suggests that SSB-1 may function to interact with MVH in the adult, whereas SSB-4 may act earlier in development, with preliminary data indicating some embryonic expression (S. E. Nicholson, unpublished data). The similarity between the SSBs is very high and with overlapping expression patterns, as in the testes, there is the possibility of functional redundancy. The phenotype of SSB-$2^{-/-}$ mice does not suggest an interaction of SSB-2 with MVH, but the analysis of compound genetic deletion of SSB family members would resolve this issue further.

SSB-2 was found to play a role in the generation of platelets and regulation of the BUN level. Although the deletion of one *Ssb-2* allele directly affects BUN levels, deletion of both alleles is required to generate thrombocytopenia. No obvious biochemical pathway links thrombocytopenia and BUN decrease. Therefore, SSB-2 may have a role in a number of different pathways through its ability to target multiple proteins for degradation. Determining the identity of these proteins could further elucidate the role of SSB-2 and the biochemical basis for the phenotypes we have observed. In conclusion, the genetic deletion of a mammalian SPRY domain-containing SOCS box protein highlights a clear role for SSB-2 both in the regulation of BUN level and in the production of platelets.

ACKNOWLEDGMENTS

This study was supported by the National Health and Medical Research Council (NHMRC) of Australia (program grant 257500), the Australian Federal Government Cooperative Research Centres Program, and AMRAD Operations Pty., Ltd., Melbourne, Australia. S.E.N. was supported by an NHMRC Biomedical Career Development award.

We thank F. Kupresanin, S. Mifsud, L. DiRago, S. Raker, C. Hyland, W. Carter, and J. Corbin for expert technical assistance and M. Carpinelli, B. Croker, and D. Krebs for helpful advice. We also thank S. Ellis for electron microscopy and T. Kemp, K. Vella, and G. Siciliano for animal experimentation and husbandry.

REFERENCES

1. **Alexander, W. S., and C. G. Begley.** 1998. Thrombopoietin in vitro and in vivo. Cytokines Cell Mol. Ther. **4:**25–34.
2. **Altschul, S. F., W. Gish, W. Miller, E. W. Myers, and D. J. Lipman.** 1990. Basic local alignment search tool. J. Mol. Biol. **215:**403–410.
3. **Berger, G., D. W. Hartwell, and D. D. Wagner.** 1998. P-selectin and platelet clearance. Blood **92:**4446–4452.
4. **Bonadio, W. A., H. H. Hennes, J. Machi, and E. Madagame.** 1989. Efficacy of measuring BUN in assessing children with dehydration due to gastroenteritis. Ann. Emerg. Med. **18:**755–757.
5. **Chang, M., Y. Suen, G. Meng, J. S. Buzby, J. Bussel, V. Shen, C. van de Ven, and M. S. Cairo.** 1996. Differential mechanisms in the regulation of endogenous levels of thrombopoietin and interleukin-11 during thrombocytopenia: insight into the regulation of platelet production. Blood **88:**3354–3362.
6. **Croker, B. A., D. L. Krebs, J. G. Zhang, S. Wormald, T. A. Willson, E. G. Stanley, L. Robb, C. J. Greenhalgh, I. Forster, B. E. Clausen, N. A. Nicola, D. Metcalf, D. J. Hilton, A. W. Roberts, and W. S. Alexander.** 2003. SOCS3 negatively regulates IL-6 signaling in vivo. Nat. Immunol. **4:**540–545.
7. **Croker, B. A., D. Metcalf, L. Robb, W. Wei, S. Mifsud, L. DiRago, L. A. Cluse, K. D. Sutherland, L. Hartley, E. Williams, J. G. Zhang, D. J. Hilton, N. A. Nicola, W. S. Alexander, and A. W. Roberts.** 2004. SOCS3 is a critical physiological negative regulator of G-CSF signaling and emergency granulopoiesis. Immunity **20:**153–165.
8. **Duarte, C. G., and H. G. Preuss.** 1993. Assessment of renal function: glomerular and tubular. Clin. Lab. Med. **13:**33–52.
9. **Elefanty, A. G., C. G. Begley, D. Metcalf, L. Barnett, F. Kontgen, and L. Robb.** 1998. Characterization of hematopoietic progenitor cells that express the transcription factor SCL, using a lacZ "knock-in" strategy. Proc. Natl. Acad. Sci. USA **95:**11897–11902.
10. **Hilton, D. J., R. T. Richardson, W. S. Alexander, E. M. Viney, T. A. Willson, N. S. Sprigg, R. Starr, S. E. Nicholson, D. Metcalf, and N. A. Nicola.** 1998. Twenty proteins containing a C-terminal SOCS box form five structural classes. Proc. Natl. Acad. Sci. USA **95:**114–119.
11. **Jackson, C. W., L. K. Brown, B. C. Somerville, S. A. Lyles, and A. T. Look.** 1984. Two-color flow cytometric measurement of DNA distributions of rat megakaryocytes in unfixed, unfractionated marrow cell suspensions. Blood **63:**768–778.
12. **Kile, B. T., D. Metcalf, S. Mifsud, L. DiRago, N. A. Nicola, D. J. Hilton, and W. S. Alexander.** 2001. Functional analysis of Asb-1 using genetic modification in mice. Mol. Cell. Biol. **21:**6189–6197.
13. **Kimura, S., A. W. Roberts, D. Metcalf, and W. S. Alexander.** 1998. Hematopoietic stem cell deficiencies in mice lacking c-Mpl, the receptor for thrombopoietin. Proc. Natl. Acad. Sci. USA **95:**1195–1200.
14. **Krebs, D. L., R. T. Uren, D. Metcalf, S. Rakar, J. G. Zhang, R. Starr, D. P. De Souza, K. Hanzinikolas, J. Eyles, L. M. Connolly, R. J. Simpson, N. A. Nicola, S. E. Nicholson, M. Baca, D. J. Hilton, and W. S. Alexander.** 2002. SOCS-6 binds to insulin receptor substrate 4, and mice lacking the SOCS-6 gene exhibit mild growth retardation. Mol. Cell. Biol. **22:**4567–4578.
15. **Kuter, D. J.** 1996. The physiology of platelet production. Stem Cells **14** (Suppl. 1)**:**88–101.
16. **Kuter, D. J., and R. D. Rosenberg.** 1995. The reciprocal relationship of thrombopoietin (c-Mpl ligand) to changes in the platelet mass during busulfan-induced thrombocytopenia in the rabbit. Blood **85:**2720–2730.
17. **Liu, J. J., J. Y. Wang, C. Zhang, A. Nilsson, and R. D. Duan.** 2002. Hepatic cirrhosis increases sensitivity of kidney to endotoxin in rats. Med. Sci. Monit. **8:**BR56–BR60.
18. **Matsumura, I., and Y. Kanakura.** 2002. Molecular control of megakaryopoiesis and thrombopoiesis. Int. J. Hematol. **75:**473–483.
19. **Metcalf, D., N. A. Nicola, and D. P. Gearing.** 1990. Effects of injected leukemia inhibitory factor on hematopoietic and other tissues in mice. Blood **76:**50–56.

20. **Neben, T. Y., J. Loebelenz, L. Hayes, K. McCarthy, J. Stoudemire, R. Schaub, and S. J. Goldman.** 1993. Recombinant human interleukin-11 stimulates megakaryocytopoiesis and increases peripheral platelets in normal and splenectomized mice. Blood **81:**901–908.
21. **Nicholson, S. E., D. De Souza, L. J. Fabri, J. Corbin, T. A. Willson, J. G. Zhang, A. Silva, M. Asimakis, A. Farley, A. D. Nash, D. Metcalf, D. J. Hilton, N. A. Nicola, and M. Baca.** 2000. Suppressor of cytokine signaling-3 preferentially binds to the SHP-2-binding site on the shared cytokine receptor subunit gp130. Proc. Natl. Acad. Sci. USA **97:**6493–6498.
22. **Ogilvy, S., A. G. Elefanty, J. Visvader, M. L. Bath, A. W. Harris, and J. M. Adams.** 1998. Transcriptional regulation of *vav*, a gene expressed throughout the hematopoietic compartment. Blood **91:**419–430.
23. **Ponting, C., J. Schultz, and P. Bork.** 1997. SPRY domains in ryanodine receptors (Ca^{2+}-release channels). Trends Biochem. Sci. **22:**193–194.
24. **Raz, E.** 2000. The function and regulation of Vasa-like genes in germ-cell development. Genome Biol. **1:**REVIEWS1017.
25. **Roberts, A. W., L. Robb, S. Rakar, L. Hartley, L. Cluse, N. A. Nicola, D. Metcalf, D. J. Hilton, and W. S. Alexander.** 2001. Placental defects and embryonic lethality in mice lacking suppressor of cytokine signaling 3. Proc. Natl. Acad. Sci. USA **98:**9324–9329.
26. **Schultz, J., F. Milpetz, P. Bork, and C. P. Ponting.** 1998. SMART, a simple modular architecture research tool: identification of signaling domains. Proc. Natl. Acad. Sci. USA **95:**5857–5864.
27. **Starr, R., D. Metcalf, A. G. Elefanty, M. Brysha, T. A. Willson, N. A. Nicola, D. J. Hilton, and W. S. Alexander.** 1998. Liver degeneration and lymphoid deficiencies in mice lacking suppressor of cytokine signaling-1. Proc. Natl. Acad. Sci. USA **95:**14395–14399.
28. **Strasser, A., A. W. Harris, and S. Cory.** 1991. bcl-2 transgene inhibits T-cell death and perturbs thymic self-censorship. Cell **67:**889–899.
29. **Styhler, S., A. Nakamura, and P. Lasko.** 2002. Vasa localization requires the SPRY-domain and SOCS-box containing protein, Gustavus. Dev. Cell **3:** 865–876.
30. **Tanaka, S. S., Y. Toyooka, R. Akasu, Y. Katoh-Fukui, Y. Nakahara, R. Suzuki, M. Yokoyama, and T. Noce.** 2000. The mouse homolog of *Drosophila* Vasa is required for the development of male germ cells. Genes Dev. **14:** 841–853.
31. **Wang, D., Z. Li, E. M. Messing, and G. Wu.** 2002. Activation of Ras/Erk pathway by a novel MET-interacting protein RanBPM. J. Biol. Chem. **277:** 36216–36222.
32. **Yao, S., S. L. Masters, J. G. Zhang, K. R. Palmer, J. J. Babon, N. A. Nicola, S. E. Nicholson, and R. S. Norton.** 2005. Backbone 1H, 13C, and 15N assignments of the 25-kDa SPRY domain-containing SOCS box protein 2 (SSB-2). J. Biomolec. NMR **31:**69–70.
33. **Yoshimura, A., T. Ohkubo, T. Kiguchi, N. A. Jenkins, D. J. Gilbert, N. G. Copeland, T. Hara, and A. Miyajima.** 1995. A novel cytokine-inducible gene CIS encodes an SH2-containing protein that binds to tyrosine-phosphorylated interleukin 3 and erythropoietin receptors. EMBO J. **14:**2816–2826.
34. **Zhang, J. G., A. Farley, S. E. Nicholson, T. A. Willson, L. M. Zugaro, R. J. Simpson, R. L. Moritz, D. Cary, R. Richardson, G. Hausmann, B. J. Kile, S. B. Kent, W. S. Alexander, D. Metcalf, D. J. Hilton, N. A. Nicola, and M. Baca.** 1999. The conserved SOCS box motif in suppressors of cytokine signaling binds to elongins B and C and may couple bound proteins to proteasomal degradation. Proc. Natl. Acad. Sci. USA **96:**2071–2076.